

## Comparison of the *in silico* antibacterial effects of coumarin-based Schiff bases and metal complexes on the DNA gyrase enzyme

Işık Çakmak<sup>a</sup> & Nurhan Gümrükçüoğlu\*<sup>b</sup>

<sup>a</sup> Biostatistics and Medical Informatics, Karadeniz Technical University, Trabzon, Türkiye

<sup>b</sup> Department of Medical Services and Techniques, Vocational School of Health Sciences, Karadeniz Technical University, Trabzon, Türkiye

E-mail: ngumrukcuoglu@ktu.edu.tr

Received 18 August 2025; accepted (revised) 11 June 2026

The global increase in antibiotic resistance is reducing the effectiveness of current treatment options and necessitating the development of new antimicrobial agents. Schiff base derivatives and metal complexes are one of the pharmacophore groups that attract attention due to their broad biological effect spectrum and high chemical stability. Metals are important components of many biochemical reactions occurring in living organisms and are among the fundamental cellular elements selected to perform various biological processes in nature. *In silico* approaches offer a significant advantage in the drug discovery process by enabling the examination of candidate molecules at low cost and in a short time. In this study, the potential inhibitory effects of the Cu (II), Zn(II), Ni(II), and Fe (II) metal complexes of the newly designed coumarin derivatives on the *Escherichia coli* DNA gyrase (PDB ID: 1KZN) enzyme were compared using molecular docking methods. The findings revealed that Schiff base metal complexes generally exhibit higher affinity than free ligands. The strongest binding was observed in the Zn-L1 (-10.6 kcal/mol) and Fe-L1/Ni-L2 (-10.3 kcal/mol) complexes. The findings suggest that Schiff base-metal complexes may be evaluated as potential antimicrobial candidates through DNA gyrase inhibition. *In vitro* studies will provide experimental evidence to support the pharmacological potential of these complexes.

**Keywords:** Schiff base metal complexes, DNA gyrase inhibition, Molecular docking, Antimicrobial resistance

Infections caused by microorganisms, especially bacteria, are among the most serious public health problems facing modern medicine. Bacteria are pathogenic microorganisms that can cause various infections in human, animal, and plant systems. The development of resistance mechanisms against antibiotics, which are widely used in the treatment of these infections, limits effective treatment options and necessitates the development of new antibacterial agents<sup>1</sup>.

The global increase in antibiotic resistance reduces the effectiveness of current treatment approaches, resulting in approximately 700,000 deaths each year, with this number projected to reach 10 million by 2050 (Ref. 2). The treatment of infections caused by resistant bacterial strains poses serious challenges both clinically and economically; complications, prolonged hospital stays, and increased mortality rates are observed during the treatment process<sup>3-6</sup>. Indeed, some pathogens, such as *Klebsiella pneumoniae*, rank among the leading causes of antibiotic-resistant deaths, further increasing the threat posed by these microorganisms<sup>7</sup>. In this regard, the discovery of new pharmaceutical agents is of

great importance in the fight against antimicrobial resistance. In recent years, Schiff base derivatives have attracted attention as pharmacologically interesting compounds due to their antibacterial, antifungal, antiviral, antiparasitic, and antioxidant properties<sup>8-13</sup>. These compounds, which have a broad biological spectrum of activity, are being evaluated as potential therapeutic agents in various biological applications<sup>14</sup>.

Researchers' interest in Schiff base ligands has grown over the years due to their ease of preparation, the greater stability of metal complexes, and their bio-organic compatibility<sup>15-18</sup>. The high stability of metal-Schiff base complexes stems from the combination of both electronic and structural factors. The nitrogen atom in the carbon-nitrogen double bond (>C=N-) of the Schiff base donates its unshared electron pair to the metal ion, forming a coordinate bond; this property forces the nitrogen to behave like a Lewis base and makes it the primary coordination point of the complex. Additionally, the  $\pi$  orbitals of the nitrogen atom overlap with the d orbitals of the metal, enabling a  $\pi$ -back-donation mechanism, which contributes to the electronic stability of the complex. Functional groups located close

to the nitrogen atom in Schiff bases, particularly the hydroxyl (–OH) group, form additional bonding sites with the metal ion, creating multi-ring (chelating) structures. This chelate effect restricts the freedom of the metal ion, ensuring that the complex is geometrically tight and stable. As a result, the coordinative ability of the nitrogen atom,  $\pi$ - $\delta$  interactions, and the combination of multiple bonding provided by functional groups determine the high stability of Schiff base-metal complexes<sup>19,20</sup>.

Schiff base metal complexes have a wide range of pharmaceutical and biological applications. Metal complexes of Schiff bases with “O” and “N” donor atoms can be cited as examples of antibacterial, antitumour, antifungal, antimalarial, enzyme inhibitors, anti-inflammatory antioxidants, antihypertensive, and anticonvulsant agents<sup>21-37</sup>. This broad range of biological effects makes *in silico* drug design techniques a fast and cost-effective method for predicting the efficacy of these complexes<sup>38</sup>.

The aim of this study is to determine the binding energies and conformational effects of metal complexes with DNA gyrase. This approach aims to evaluate the potential antimicrobial activity of metal complexes and their comparative interaction profiles with ligands. In

this context, the effects of Cu(II), Zn(II), Ni(II), and Fe(II) metal complexes with coumarin-based Schiff bases on the *Escherichia coli* DNA gyrase enzyme were investigated using molecular docking studies.

### Molecular Docking study

*In-silico* simulations were performed using AutoDock Vina<sup>39</sup> software. The DNA gyrase protein from *Escherichia coli* (PDB ID: 1KZN) was used in the study. The protein structure was obtained from the RCSB PDB database<sup>40</sup>. Prior to the simulation, all water molecules, cofactors, and co-crystal ligands associated with the protein were removed. AutoDock Tools<sup>41</sup> and UCSF Chimera<sup>42</sup> software were used to prepare the receptor and co-crystal structures. The grid box dimensions and centre were set as follows: centre\_x = 19.0, centre\_y = 31.041, centre\_z = 34.027, size\_x = 22, size\_y = 22, size\_z = 22, num\_modes = 10. The ligands (L1 and L2) used in the study were designed and are original molecules not found in the literature. The 2D structures of the ligands were drawn using Chemical Sketch Tool<sup>43</sup>, and then geometry optimisations were performed in Avogadro<sup>44</sup> and saved in 3D format. The 2D and 3D visuals of the structures are provided in Fig. 1.

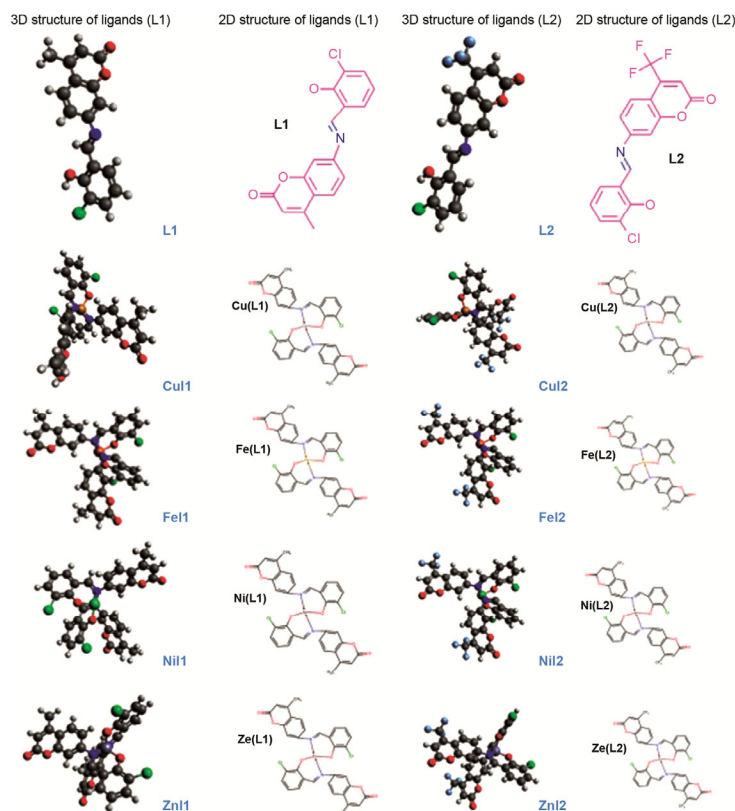


Fig. 1 — Two-dimensional (2D) and three-dimensional (3D) images of structures

The structures obtained were converted to pdbqt format using Open Babel<sup>45</sup> software. The results obtained after molecular docking were evaluated in terms of binding energies and interaction types. Discovery Studio<sup>46</sup>, Chimera<sup>42</sup>, and PyMOL<sup>47</sup> software were used for the interpretation and visualisation of the results. To test the accuracy of the method, a re-docking study was performed with the crystallised ligand, and the obtained structure was superimposed on the crystal structure and visualised using PyMOL<sup>47</sup> software (Fig. 2).

### Results and Discussion

Molecular docking studies were performed on the 1KZN-coded protein receptor with L1 and L2 ligands and their Cu(II), Fe(II), Ni(II) and Zn(II) metal complexes. The main amino acids in the active site of the 1KZN receptor are ARG136, ASP73, ASN46, GLY77, ARG76, GLU50, THR165, ALA47, ILE90, PRO79, and VAL71, and hydrogen bonds, halogen,

electrostatic, and hydrophobic interactions were observed in this region. The binding affinity of the co-crystal ligand was calculated as  $-9.3$  kcal/mol. The conformational states of the L1 and L2 ligands within the receptor are shown in Fig. 3.

According to the results of the L1 series; The binding affinity of the CuL1 complex is  $-10.4$

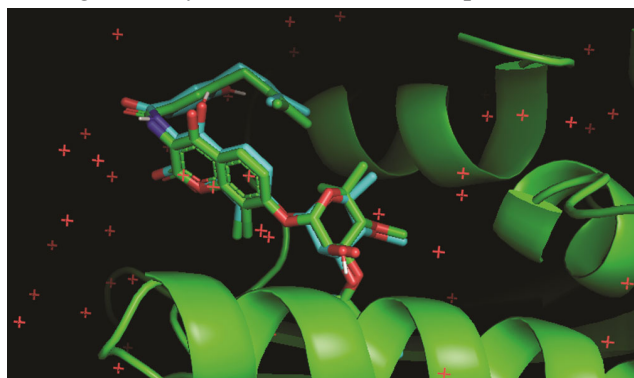


Fig. 2 — Visualisation of docking analysis with crystallised ligand structure (re-dock)

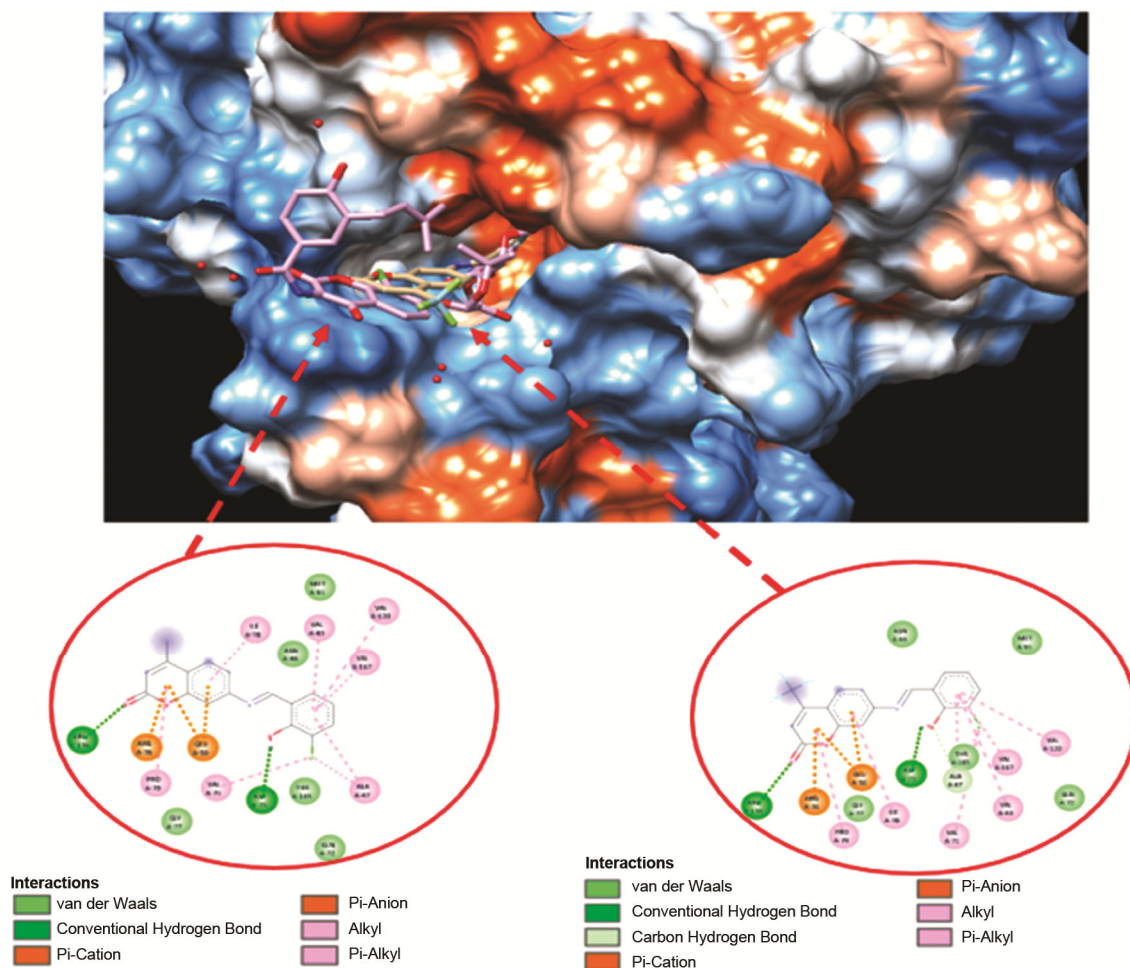


Fig. 3 — Conformations of L1 and L2 ligands within the receptor

kcal/mol, and it exhibits hydrogen bonds with ARG76, ARG136, and ASN46 in the active site, electrostatic interactions with ASP49 and ARG76, and hydrophobic contacts with amino acids such as ILE78, ILE90, VAL120, PRO79, and ALA53. The FeL1 complex has a binding affinity of -10.3 kcal/mol and forms hydrogen bonds with VAL120, SER121, and ALA47, electrostatic interactions with ARG76 and GLU50, and hydrophobic contacts with ILE90, MET91, and VAL120. The NiL1 complex exhibits a binding affinity of -9.2 kcal/mol, forming hydrogen bonds with ASN46, ARG76, and THR165, electrostatic interactions with ASP49 and GLU50, and hydrophobic contacts with ILE78, PRO79, ILE90, and ALA96. The ZnL1 complex exhibits electrostatic interactions with ASP49 and ARG76, hydrogen bonds with ASN46 and ARG136, and hydrophobic contacts with ILE78, ILE90, VAL120, and PRO79, with a binding affinity of -10.6 kcal/mol. The free L1 ligand forms hydrogen bonds with ARG136 and ASP73 and electrostatic interactions with ARG76 at -8.6 kcal/mol (Fig. 3, Table 1, Table 2 and Table 3).

When the L2 series is examined, the CuL2 complex exhibits hydrogen bonds with ARG76 and ARG136 with a binding affinity of -10.1 kcal/mol, halogen and electrostatic interactions with ASP49, electrostatic interactions with GLU50, and hydrophobic contacts with ILE78, ILE90, ALA53, etc. The FeL2 complex exhibits a binding affinity of -10.0 kcal/mol with hydrogen bonds with VAL120, THR165, and ALA47, halogen interactions with

ASN46 and ASP73, electrostatic contacts with ARG76, and hydrophobic interactions with MET91, ILE90, and ILE78. The NiL2 complex exhibits a binding affinity of -10.3 kcal/mol with VAL120, THR165, and ALA47, electrostatic interactions with ARG76 and GLU50, halogen bonds with amino acids such as ASP73, HIS95, and ASN46, and hydrophobic contacts with ALA53 and ILE90. ZnL2 complex -9.7 kcal/mol binding affinity with hydrogen bonds with ASP49, ASN46, and THR165, hydrogen and halogen interactions with GLY77 and VAL120, and hydrophobic contacts with ILE78, ILE90, and PRO79. The free L2 ligand exhibits hydrogen bonds with ARG136 and ASP73, electrostatic contacts with ARG76, and hydrophobic interactions with amino acids such as ALA47, VAL71, and ILE78, with a binding affinity of -8.4 kcal/mol (Fig. 1, Table 1, Table 2 and Table 3).

Table 1 — Binding energies obtained as a result of molecular docking

Ligand	Energy Values (kcal/mol)
Ikzn_cocrystal	-9.3
CuL1	10.4
CuL2	-10.1
FeL1	-10.3
FeL2	-10
L1	-8.6
L2	-8.4
NiL1	-9.2
NiL2	-10.3
ZnL1	-10.6
ZnL2	-9.7

Table 2 — Amino Acid Interaction Table (L1 Series)

Cu-L1	Type of Interaction	Fe-L1	Type of Interaction	Ni-L1	Type of Interaction	Zn-L1	Type of Interaction	1KZN-L1	Type of Interaction
ARG76	Hydrogen Bond	VAL120	Hydrogen Bond	ASN46	Hydrogen Bond	ASP49	Electrostatic	ARG136	Hydrogen Bond
ARG136	Hydrogen Bond	SER121	Hydrogen Bond	ARG76	Hydrogen Bond	ARG76	Hydrogen Bond	ASP73	Hydrogen Bond
ARG76	Electrostatic	ALA47	Hydrogen Bond	THR165	Hydrogen Bond	ARG136	Hydrogen Bond	ARG76	Electrostatic
ASP49	Electrostatic	ARG76	Electrostatic	ASP49	Electrostatic	ARG76	Electrostatic	GLU50	Electrostatic
ASN46	Hydrogen Bond	GLU50	Electrostatic	GLU50	Electrostatic	ASN46	Hydrogen Bond	ALA47	Hydrophobic
ASN46	Hydrophobic	ASN46	Hydrogen Bond	ILE78	Hydrophobic	ASN46	Hydrophobic	VAL71	Hydrophobic
ILE78	Hydrophobic	ILE90	Hydrophobic	PRO79	Hydrophobic	ILE78	Hydrophobic	ILE78	Hydrophobic
ILE90	Hydrophobic	ILE78	Hydrophobic	ILE90	Hydrophobic	ILE90	Hydrophobic	PRO79	Hydrophobic
VAL120	Hydrophobic	MET91	Hydrophobic	ALA96	Hydrophobic	VAL120	Hydrophobic	VAL43	Hydrophobic
PRO79	Hydrophobic	VAL120	Hydrophobic			ILE78	Hydrophobic	VAL120	Hydrophobic
ALA53	Hydrophobic	VAL167	Hydrophobic			PRO79	Hydrophobic	VAL167	Hydrophobic
		ALA53	Hydrophobic			ALA53	Hydrophobic		
		ILE78	Hydrophobic						

Table 3 — Amino Acid Interaction Table (L2 Series)

Cu-L2	Type of Interaction	Fe-L2	Type of Interaction	Ni-L2	Type of Interaction	Zn-L2	Type of Interaction	1KZN-L2	Type of Interaction
ARG76	Hydrogen Bond	VAL120	Hydrogen Bond	VAL120	Hydrogen Bond	ASP49	Electrostatic	ARG136	Hydrogen Bond
ARG136	Hydrogen Bond	THR165	Hydrogen Bond	THR165	Hydrogen Bond	ASN46	Hydrogen Bond	ASP73	Hydrogen Bond
ASP49	Halogen	ALA47	Hydrogen Bond	ALA47	Halogen	ASN46	Halogen	ALA47	Hydrogen Bond
ARG76	Electrostatic	HIS95	Hydrogen Bond	ALA47	Hydrogen Bond	GLY77	Hydrogen Bond	ARG76	Electrostatic
ASP49	Electrostatic	ASN46	Halogen	HIS95	Hydrogen Bond	VAL120	Hydrogen Bond	GLU50	Electrostatic
GLU50	Electrostatic	ASP73	Halogen	HIS95	Halogen	VAL120	Halogen	ALA47	Hydrophobic
ASN46	Hydrogen Bond	HIS95	Halogen	THR165	Halogen	THR165	Hydrogen Bond	VAL71	Hydrophobic
ASN46	Hydrophobic	ARG76	Electrostatic	ASN46	Halogen	GLY119	Hydrogen Bond	ILE78	Hydrophobic
ALA53	Hydrophobic	GLU50	Electrostatic	ASP73	Halogen	ILE90	Halogen	PRO79	Hydrophobic
ILE78	Hydrophobic	ASN46	Hydrogen Bond	HIS95	Halogen	GLY119	Halogen	VAL43	Hydrophobic
ILE90	Hydrophobic	ALA53	Hydrophobic	ARG76	Electrostatic	ILE78	Hydrophobic	VAL120	Hydrophobic
MET91	Hydrophobic	ILE90	Hydrophobic	GLU50	Electrostatic	ILE90	Hydrophobic		
VAL120	Hydrophobic	ILE78	Hydrophobic	ASN46	Hydrogen Bond	PRO79	Hydrophobic		
PRO79	Hydrophobic	ALA47	Halogen	ALA53	Hydrophobic	ILE78	Hydrophobic		
ILE90	Hydrophobic	THR165	Halogen	ILE90	Hydrophobic				

The obtained data show that there is a significant increase in binding affinity and binding energy with the coordination of metal ions to both L1 and L2 ligands.

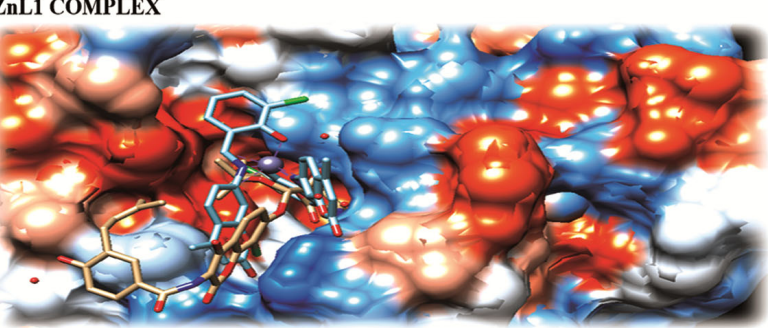
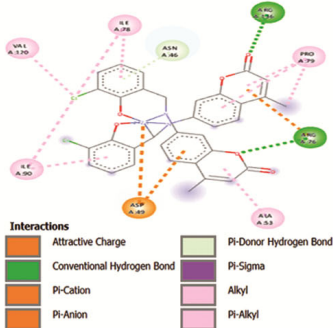
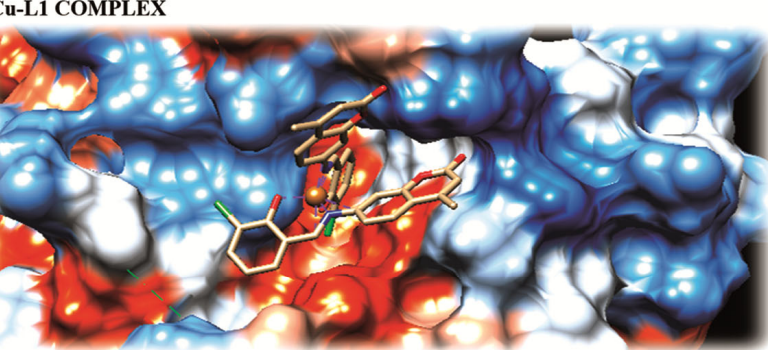
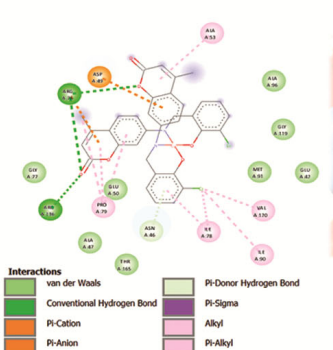
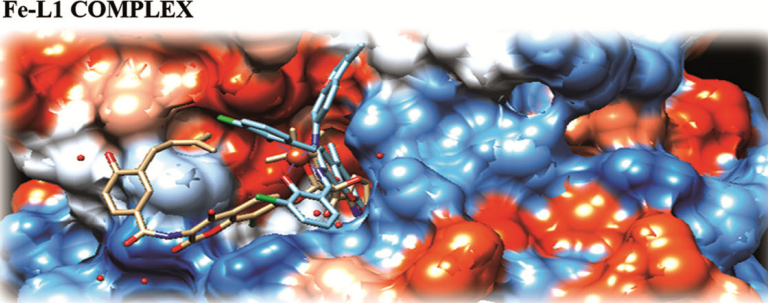
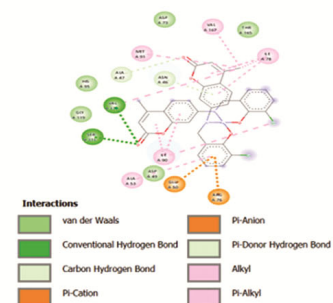
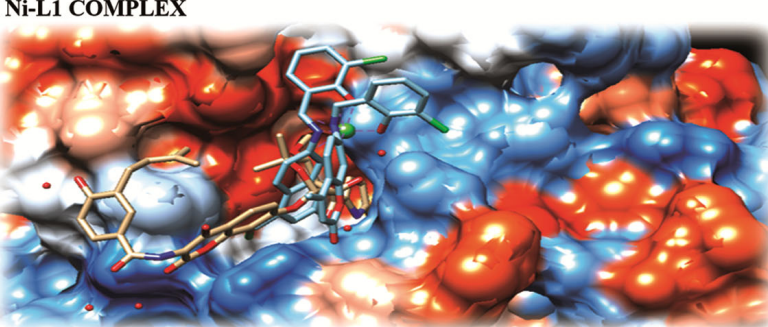
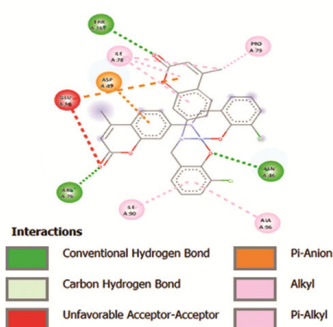
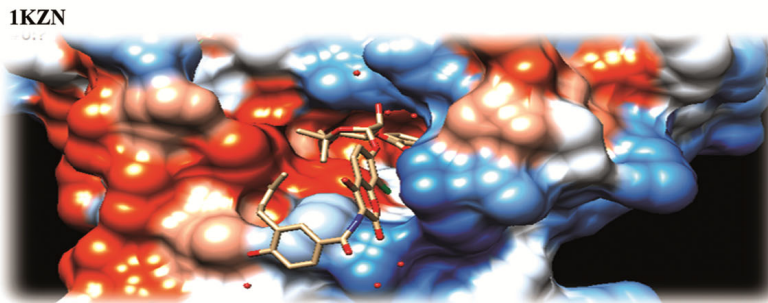
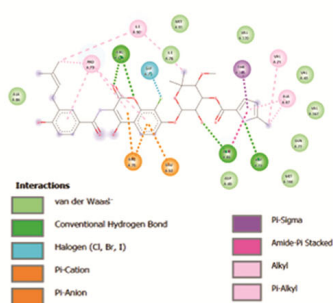
Compared to free ligands, all metal complexes exhibited higher (more negative) binding energy values, indicating that complexation increases the binding strength to the receptor. In particular, the ZnL1 (−10.6 kcal/mol) and NiL2 (−10.3 kcal/mol) complexes stand out as having the strongest inhibitory potential against the active site of the 1KZN receptor (Fig. 4, Table 1).

Molecular docking studies are critical tools for predicting the interactions of metal complexes with DNA and protein-like biomolecules. In a study, docking analyses conducted on VO(II), Fe(III), Co(II), Ni(II) and Cu(II) complexes obtained with Fe(III), Co(II), Ni(II) and Cu(II) demonstrated that the complexes bind to DNA with high stability and affinity through both hydrogen bonds and hydrophobic interactions<sup>48</sup>. Similarly, studies conducted on indole-thiosemicarbazone ligands and Fe(III)-, Co(II)-, Ni(II)-, and Cu(II)- complexes also emphasise the importance of docking analyses in the interaction of these complexes with bacterial targets. Docking results are generally consistent with *in vitro*

findings, and complexes with high binding energy are also found to have high biological activity. Therefore, molecular docking is an important predictive tool supporting the therapeutic potential of metal complexes<sup>49</sup>. Additionally, DFT and docking analyses of heteroleptic metal(II)-thiosemicarbazone complexes have shed light on their antibacterial effects and interaction models with cellular target proteins; this suggests that molecular docking enhances the reliability of providing insights into biological activity<sup>50</sup>.

In another study by Schiff on certain ligands and transition metal complexes, biological effect studies based on both DNA binding and docking analyses were conducted after these compounds formed complexes with VO(II), Zn(II) and ZrO(II) (Ref. 51). In another study, the antibacterial and anticancer potentials of mixed ligand–metal complexes were evaluated and supported by docking analyses<sup>52</sup>.

In our study, metal ligand complexes were designed based on the findings (data) of the studies and evaluated using *in silico* methods in terms of antibacterial activity. The antibacterial activities of coumarin-derived Schiff bases against *Escherichia coli* DNA gyrase enzyme have significantly increased with the formation of metal complexes. Improvements



(Contd.)

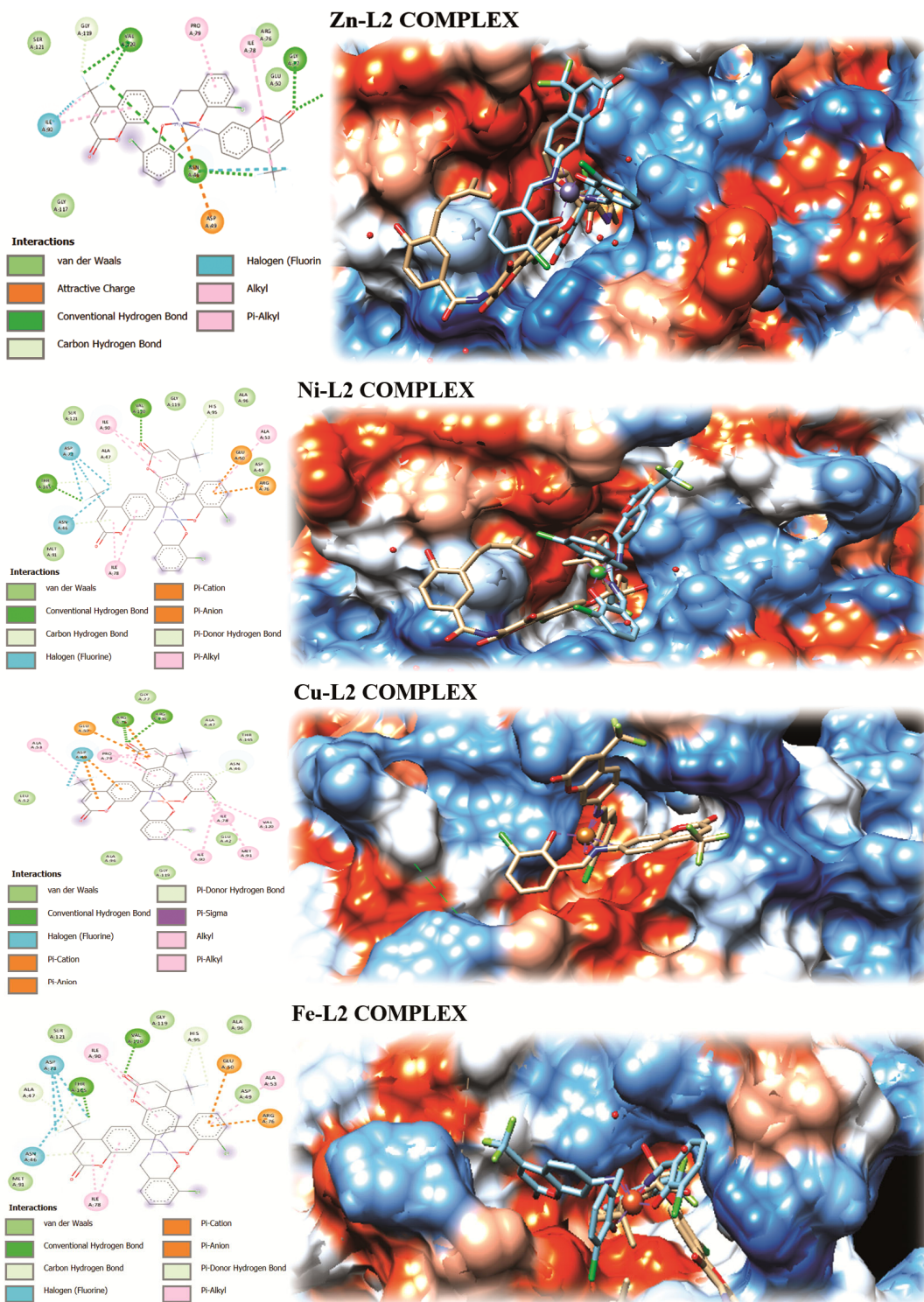


Fig. 4 — Conformations and binding states of ligand complexes within the receptor

in biological activity have been observed in metal complexes.

It has been determined that the designed coumarin-based Schiff bases exhibit antibacterial effects comparable to the co-crystal ligand structure used as a

reference. The potential of metal complexes to enhance biological activity is significant because they can be synthesised in a single step and prepared using environmentally friendly (green synthesis) methods. However, comprehensive *in vitro* studies must be

conducted before any potential pharmaceutical applications.

## References

- Pancu D F, Scurtu A, Macasoï I G, Marti D, Mioc M, Soica C, Coricovac D, Horhat D, Poenaru M & Dehelean C, *Antibiotics*, 10 (2021) 401.
- Ventola C L, *Pharm Therap*, 40 (2015) 277.
- Marchese A, Barbieri R, Sanches-Silva A, Daglia M, Nabavi S F, Jafari N J & Nabavi S M, *Trends Food Sci & Tech*, 52 (2016) 49.
- Barbieri R, Coppo E, Marchese A, Daglia M, Sobarzo-Sánchez E, Nabavi S F & Nabavi S M, *Microbio Res*, 196 (2017) 44-68.
- Vivas R, Barbosa A A T, Dolabela S S & Jain S, *Microbial Drug Resistance*, 25 (2019) 890.
- Mühlberg E, Umstätter F, Kleist C, Domhan C, Mier W & Uhl P, *Canadian J Microbiology*, 66 (2020) 11.
- Murray C J, Ikuta K S, Sharara F, Swetschinski L, Aguilar G R, Gray A & Tasak N, *Lancet*, 399 (2022) 629.
- Salama H E, Saad G R & Sabaa M W, *Int J Bio Macromol*, 79 (2015) 996.
- Mesbah M, Douadi T, Sahli F, Issaadi S, Boukazoula S & Chafaa S, *J Mol Struct*, 1151 (2018) 41.
- Kaur H, Lim S M, Ramasamy K, Vasudevan M, Shah S A A & Narasimhan B, *Arabian J Chem*, 13 (2020) 377.
- Khadra K A, Mizyed S, Marji D, Haddad S F, Ashram M & Foudeh A, *Spectrochim Acta Part A: Mol Biomol Spect*, 136 (2015) 1869.
- Süleymanoğlu N, Ustabas R, Direkel Ş, Alpaslan Y B & Ünver Y, *J Mol Struct*, 1150 (2017) 82.
- Thakkar S S, Thakor P, Doshi H & Ray A, *Bioorg Med Chem*, 25 (2017) 4064.
- Abdel-Rahman L H, Abu-Dief A M, Aboelez M O & Abdel-Mawgoud A A H, *J Photochem Photobio B: Bio*, 170 (2017) 271-285.
- Poornima K, Kosuru R Y & Srinivasan V, *Chem Sel*, 10 (2025) e00134.
- Alnajeebi A M, Shafie A, Alubaidi A, Ashour A A, Felemban M F & Tayeb F J, *J Fluorescence*, 35 (2025) 7227.
- Iacopetta D, Catalano A, Ceramella J, Mariconda A, D'Amato A, Checconi P & Sinicropi M S, *Molecules*, 30 (2025) 207.
- Triviño-Rojas M K, Jiménez-Lopez S J, D'Vries R, Aragón-Muriel A & Polo-Cerón D, *Inorganics*, 13 (2025) 213.
- Thakur S, Jaryal A & Bhalla A, *Results Chem*, 7 (2024) 101350.
- Mezgebe K & Mulugeta E, *Med Chem Res*, 33 (2024) 439.
- Tchekalarova J, Stoyanova T & Todorov P, *Curr Res Biotech*, 10 (2025) 100317.
- Tawfiq K M, Al Naymi H A S, Obaid S M, Jarad A J, Al-Noor T H & Al-Sarray A J, *App Organomet Chem*, 39 (2025) e7781.
- Buran K, *J Mole Struct*, 1330 (2025) 141499.
- Elazoomi N H E, *Libyan J Med App Sci*, 3 (2025) 59.
- Oveysi Keikha A, Shahraki S, Dehghanian E, Mansouri-Torshizi H, *J Mol Liq*, 391 (2023) 123272.
- Taha R H, Saleh A M, Abbass L M, El-Fakharany E M, Almutlq N J, Hussein M F & Moustafa S M, *J Mol Liq*, 427 (2025) 127382.
- Murugan T, Venkatesh R, Imran P M, Kubaib A, Alnjaa A A & Abdellattif M H, *J Mol Liq*, 423 (2025) 126987.
- Kumar B, Devi J, Chetna & Taxak B, *Res Chem Intermed*, 51 (2025) 411.
- Taxak B, Devi J, Kumar B & Rani M, *J Mol Struct*, 1322 (2025) 140309.
- Peron C, Gonçalves R S B & Moura S, *App Organomet Chem*, 39 (2025) e70050.
- Turan N, Kızılkaya S, Buldurun K, Çolak N, Akdeniz A & Bursal E, *J Mol Struct*, 1338 (2025) 142167.
- Michael S, Jeyaraman P, Jancy J V, Muniyandi V & Raman N, *Int J Biological Macromole*, 306 (2025) 141760.
- Dhanya T M, Kurup M P, Rajimon K J, Krishna G A, Varughese J K, Raghu K G & Mohanan P V, *Dalton Trans*, 54 (2025) 3216.
- Keikha A O, Shahraki S, Dehghanian E & Mansouri-Torshizi H, *Spectrochim Acta Part A: Mole Biomol Spect*, 325 (2025) 125034.
- Michael S, Jeyaraman P, Marimuthu B & Raman N, *App Organomet Chem*, 39 (2025) e7877.
- Subhan Z, Ali N, Ullah A, Ali W, Nabi M & Shah S W A, *Biomolecules*, 15 (2025) 611.
- Paul S & Barman P, *Dalton Trans*, 54 (2025) 2132-2146.
- Chang Y, Hawkins B A, Du J J & Groundwater P W, *Pharmaceutics*, 15 (2022) 49.
- Trott O & Olson A J, *J Comp Chem*, 31 (2010) 455.
- Berman H M, Westbrook J, Feng Z, Gilliland G, Bhat T N & Weissig H, *Nucleic Acids Res*, 28 (2000) 235.
- Morris G M, Huey R, Lindstrom W, Sanner M F, Belew R K, Goodsell D S & Olson A J, *J Comp Chem*, 30 (2009) 2785.
- Pettersen E F, Goddard T D, Huang C C, Couch G S, Greenblatt D M, Meng E C & Ferrin T E, *J Comp Chem*, 25 (2004) 1605.
- RCSB Protein Data Bank, Chemical Sketch Tool, ChemAxon. <https://www.rcsb.org/>.
- Hanwell M D, Curtis D E, Lonie D C, Vandermeersch T, Zurek E & Hutchison G R, *J Cheminform*, 4 (2012) 17.
- O'Boyle N M, Banck M, James C A, Morley C, Vandermeersch T & Hutchison G R, *J Cheminfo*, 3 (2011) 33.
- BIOVIA, Dassault Systèmes, Discovery Studio Visualizer (Version 21.1) [Software], San Diego: Dassault Systèmes (2020).
- Schrödinger L & DeLano W, PyMOL. <http://www.pymol.org/pymol> (2020).
- AlZamil N O, *Mat Res Exp*, 7 (2020) 065401.
- Singh J, Gautam S, Singh M B, Singh P & Kumar U, *Chem Biodiversity*, 21 (2024) e202401301.
- Abdalla E M, Hassan S S, Elganzory H H, Aly S A & Alshater H, *Molecules*, 26 (2021) 5851.
- Abdel-Rahman L H, Al-Farhan B S, Al Zamil N O, Noamaan M A, Ahmed H E S & Adam M S S, *Bioorg Chem*, 114 (2021) 105106.
- Khan T, Zehra S, Fatima U, Mishra N, Lawrence R, Maurya A, Singh S, Jeyakumar E & Raza S, *Chem Africa*, 1-18 (2023). <https://doi.org/10.1007/s42250-023-00640-453>.